Water-Rock Interaction – Birkle & Torres-Alvarado (eds)
© 2010 Taylor & Francis Group, London, ISBN 978-0-415-60426-0

Correlation between particle size and surface area for chlorite and K-feldspar

I.E. Dubois
Industrial Ecology, Royal Institute of Technology, KTH, Stockholm, Sweden
Nuclear Chemistry, Chalmers University of Technology, Gothenburg, Sweden

S. Holgersson & S. Allard
Nuclear Chemistry, Chalmers University of Technology, Gothenburg, Sweden

M.E. Malmström
Industrial Ecology, Royal Institute of Technology, KTH, Stockholm, Sweden

ABSTRACT: The specific surface area as determined by BET analysis is often used for scaling mineral surface reaction capacities and rates between particles of different sizes as found in nature. Generally, an inverse proportionality between BET area and particle size is assumed, based on geometry. However, macroscopic laboratory studies of mineral surface reactions generally employ crushed material that may have been mechanically disturbed, potentially leading to an artificial increase in the specific surface area, and a change in the apparent surface reactivity. In this study, we determine the BET area for natural K-feldspar and chlorite samples from Sweden as function of particle size in a first step towards relating the surface reactivity for these minerals to grain size.

1 INTRODUCTION

Interactions of mineral surfaces with the aqueous solution represent a key control on many geochemical processes of environmental relevance. This is manifested for instance by the relation of such reactions to the safety of deep repositories for nuclear wastes, facilities for geological storage of carbon dioxide, and deposits for mining waste. Mineral dissolution upon weathering may alter the chemical condition and/or provide redox and pH buffering capacity. The minerals may also sorb metals/pollutants, thereby reducing the spreading of these substances from the source.

In nature, minerals can occur as particles of various sizes. As a first order approximation, the specific surface area is often used to scale surface reaction capacities or rates between particles of different sizes (e.g. White and Peterson 1990). However the proportionality between surface reactivity and specific surface area is a subject of debate in the literature (e.g. Hodson 1999, 2006; Gautier et al. 2001; Rozalen et al. 2008; Zazzi et al. 2010).

Laboratory quantification of the surface reactions usually employs crushed material. In macroscopic studies, it is often assumed that there is an inverse proportionality between surface area and particle size (e.g. Brandt et al. 2003). However, Byegård et al. (1998) and André et al. (2009) for granite and Dubois et al. (2010) for natural magnetite and labradorite, have observed a deviation from linearity when relatively large particle size fractions are considered. André et al. (2009) proposed that this was due to artificial, new surfaces associated with newly developed microcracks within a mechanically disturbed zone at the particle edge.

This work aims at studying the dependency of the specific surface area, measured via the BET method, and the particle size for two common silicate minerals, chlorite and K-feldspar.

2 THEORY

André et al. (2009) developed a model to represent the dependency of the specific surface area on the particle size for spherical particles. Here, we modified this approach to parallelepiped shaped particles, as SEM investigations showed that this was a more realistic geometry for feldspar and particularly chlorite. For a parallelepiped with the sides a, b and c, where $a = lb$ and $c = mb$, $l > 1$ and $m < 1$, the parameter b will determine which size fraction the particle ends up in upon sieving. Thus, we use b as the characteristic size of the particle.

The external specific surface area of such a particle is:

$$SSA_{ext} = \frac{2\lambda \cdot (ab + ac + bc)}{abc \cdot \rho} = \frac{2\lambda\beta}{\rho} \cdot \frac{1}{b} \quad (1)$$

where λ [-] is the roughness factor, representing the deviation from a perfectly smooth surface; ρ[g.m^{-3}] is the density of the studied material, and β is a form factor defined as $\beta = 1 + l^{-1} + m^{-1}$.

For a cubic particle, $\beta = 3$, whereas an elongated or platy form of the particle yields $2 \leq \beta \leq 3$ and $\beta > 3$, respectively.

The internal surface area can be expressed by

$$SSA_{\text{int}} = \frac{\alpha_{\text{int}}}{\rho} \quad (2)$$

where α_{int} [m^2.m^{-3}] represents the internal surface area per mineral volume.

The mechanical processing of the rock (drilling, sawing, and crushing) creates a disturbed zone, millimeter to centimeter thick (Anbeek 1992). New surfaces created by the mechanical processing are then included in the surface area measurements, in addition to naturally present surfaces. The created surface is taken in account in the model, by introducing an additional internal surface area, SSA_{dist}.

$$SSA_{dist} = \frac{\alpha_{dist}}{\rho} \quad (3)$$

where α_{dist} [m^2.m^{-3}] represents the contribution of the internal surface area per mineral volume, due to the mechanical disturbance.

In the case of small particles, $c \leq 2\delta$, the disturbed zone extends throughout the whole particle and the measured surface area is linearly dependent on the inverse of the particle size.

$$SSA_{tot} = \frac{2\lambda\beta}{b\rho} + \frac{\alpha_{\text{int}}}{\rho} + \frac{\alpha_{\text{dist}}}{\rho} \quad (4)$$

However, for large particles, there is a deviation from this linear trend, as only part of the particle is mechanically disturbed (Fig. 1).

$$SSA_{tot} = \frac{2\lambda\beta}{b\rho} + \frac{\alpha_{\text{int}}}{\rho} + \frac{\alpha_{dist}}{\rho}\left[2\frac{\delta}{b}\left(1 + \frac{1}{l} + \frac{1}{m}\right) - \left(2\frac{\delta}{b}\right)^2\left(\frac{1}{lm} + \frac{1}{l} + \frac{1}{m}\right) + \left(2\frac{\delta}{b}\right)^3 \frac{1}{lm}\right] \quad (5)$$

where δ [m] represents the thickness of the disturbed zone, which is assumed to be constant over the whole particle.

Figure 1. Conceptual view of the distribution of the internal surface area for four different particle sizes. The black part represents the disturbed zone and the grey part represents the undisturbed volume. The smallest particles consist entirely of disturbed zone.

For geometrically similar particles within a certain range of size (Fig. 1), and by assuming a rectangular distribution of the particle sizes between the lower and upper sieve cutoffs, b_1 and b_2, the inverse representative particle size can be calculated as (cf. André et al. 2009)

$$b_{rep}^{-1} = \frac{4 \cdot (b_2^3 - b_1^3)}{3 \cdot (b_2^4 - b_1^4)} \quad (6)$$

3 MATERIAL AND METHODS

3.1 *Minerals*

Chlorite is a phyllosilicate, commonly found in metamorphic rocks and it occurs also as a weathering or hydrothermal alteration product of some mafic silicates, such as pyroxenes, amphiboles or biotites. The sample used in this study, from Falun, Sweden, belongs to the clinochlore sub-family.

Feldspars are tectosilicates and the most abundant mineral group (about 60%) in the Earth's crust. The particular sample used here is a potassium feldspar, sanidine, from the archipelago outside Stockholm, Sweden.

3.2 *Mineral analysis*

The purity of the minerals was confirmed with XRD analyses. Results of the chemical analyses (ICP-OES or ICP-AES –QMS or –SMS after chemical digestion) and density measurements are summarized in Table 1.

The tentative mineral compositions of the chlorite is $(Mg_{3.08}Fe_{2.26})(Si_{2.53}Al_{2.38})O_{10}(OH)_8$ and of the sanidine is $(K_{0.82}Na_{0.25}Fe_{0,01})(Si_{2.92}Al_{1.07})O_8$, based on the results in Table 1.

3.3 *Experimental methods*

The material was first roughly broken up with a hammer, and then mechanically crushed with a pestle in an agate mortar. The crushed material was then sieved (Retsch stainless steel sieves, 200 mm Ø 250 and/or 500 mm) on a shaking machine. Seven fractions were collected: 0.075–0.125; 0.125–0.250; 0.250–0.500; 0.500–1.0; 1.0–2.0; 2.0–4.0 and 4.0–8.0 mm. The fractions were then washed with 95% ethanol until

Table 1. Chemical composition and density (ρ) for chlorite and feldspar samples.

Element [%wt]	Chlorite	Feldspar
SiO_2	23.9	62.8
Al_2O_3	19.1	19.6
CaO	0.2	0.198
Fe_2O_3	28.4	0.261
K_2O	<0.06	13.8
MgO	19.5	<0.02
Na_2O	<0.05	2.73
P_2O_5	0.047	1.35
C	<0.1	<0.1
S	0.06	n.d.
ρ (kg/L)	2.85	2.71

n.d.-not determined.

ultrafine particles were removed, as indicated by the clarity of the ethanol. SEM pictures confirmed the removal of the small particles.

Ten-points BET specific surface area measurements (ASAP 2020, Micromeritics) were made on the collected size fractions, with Kr as the adsorbing gas. The samples were degassed under high vacuum for 25h at room temperature prior to the measurement. The specific surface area [$m^2.kg^{-1}$] was multiplied by the mineral's density [$kg.m^{-3}$] in order to obtain comparable results for the two minerals.

4 RESULTS AND DISCUSSION

Figure 2 shows the specific surface area of the sanidine as a function of the inverse of the characteristic particle size. For the particle sizes studied (0.075–8.0 mm), there is a linear dependency of SSA_{tot} on b^{-1}. Tentatively, we interpret this as a result of the form factor and the internal surface area being both constant over the particle sizes. Considering slightly elongated particles, as indicated by SEM and optical microscopy inspection of some samples of various particle sizes, this gives an apparent surface roughness factor of 4–5, which is within the range reported for the sanidine specimen studied by Hodson (1999).

For chlorite, two linear trends of the BET surface area as function of the inverse of the representative particle size were observed (Fig. 3). Two additional particle size fractions (0.075–0.053 and 0.053–0.025 mm) were measured to confirm the results. Those two trends indicate a difference in particle geometry, internal surface area or surface roughness between the two ranges of particle sizes studied. We note that the specific surface area of the smallest particles (0.025–0.250 mm) is less strongly dependent on the particle size than that of the larger particles (0.250–8.0 mm). Based on an assumed platy shape of the chlorite particles, this may imply that the small particles are smoother or relatively less thin than the larger particles. Two similar linear trends were observed also for magnetite over the particle size range 0.075–8.0 mm in a previous study (Dubois et al. 2010). Further investigations are needed to understand this phenomenon.

We note that for the 0.075–0.125 mm size fraction, which is often used in macroscopic laboratory studies of surface reactions, the internal surface makes up only around 10% (sanidine) to 45% (chlorite) of the total surface.

In Figures 4 and 5, we compare results from this study with data from the literature. We conclude that even though the specific surface area varies from one

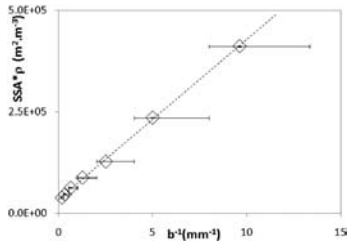

Figure 2. BET surface area [$m^2.m^{-3}$] as a function of the inverse of the particle size [mm^{-1}] for sanidine. Note that the horizontal error bars represent the range of the selected particle size fraction. Linear regression of Eq. 4 to data yields to $\lambda\beta \approx 19$ and $(\alpha_{int}+\alpha_{dist}) \approx 3.6 \times 10^4$ $m^2.m^{-3}$.

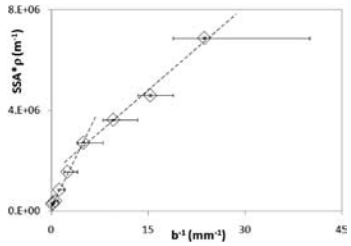

Figure 3. BET surface area [$m^2.m^{-3}$] as a function of the inverse of the particle size [mm^{-1}] for chlorite. Note that the horizontal error bars represent the range of the selected particle size fraction. Linear regressions of Eq. 4 to data yield $\lambda\beta \approx 90$ and $(\alpha_{int}+\alpha_{dist}) \approx 2.0 \times 10^6$ $m^2.m^{-3}$ for the finest particles and $\lambda\beta \approx 260$ and $(\alpha_{int}+\alpha_{dist}) \approx 1.7 \times 10^5$ $m^2.m^{-3}$ for the larger particles.

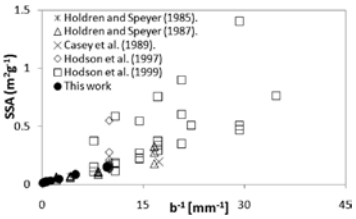

Figure 4. Specific surface area of sanidine as a function of the inverse of the particle size. Data from this study and the literature.

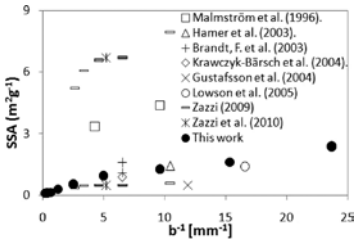

Figure 5. Specific surface area of chlorite as a function of the inverse of the particle size. Data from this study and the literature.

specimen to another, results obtained in this work are generally in good agreement with literature data.

5 CONCLUSIONS

Results of BET area measurements on chlorite and sanidine over a range of particle sizes (0.025 and 0.075 to 8.0 mm) showed that with decreasing particle size, the surface area increases. For sanidine, an inverse proportionality between BET surface area and particle size was observed, whereas for chlorite two regions with different behavior were observed. We suggest that for the particle size 0.075–0.125 mm, often employed in macroscopic laboratory studies of mineral surface reactions, the pristine surface not produced by mechanical treatment is just a small fraction of the total surface area as determined by BET analysis.

ACKNOWLEDGEMENTS

We acknowledge Karl-Erik Perhans, Geo Läromedel, Sollentuna, Sweden, for providing the mineral samples; Britt-Marie Steenari, Environmental Inorganic Chemistry and Industrial Materials Recycling Departments, Chalmers, for XRD measurements; Kristian Larsson, Industrial Materials Recycling Department, Chalmers, for SEM investigations and the Swedish Nuclear Fuel and Waste Management Co, SKB, Stockholm, Sweden for financial support.

REFERENCES

Anbeek, C. 1992. Surface roughness of minerals and implications for dissolution studies. *Geochimica et Cosmochimica Acta* 56: 1461–1469.

André, M., Malmström, M.E. & Neretnieks, I. 2009. Specific surface area measurements on intact drillcores and evaluation of extrapolation methods for rock matrix surfaces. *Journal of Contaminant Hydrology* 110(1): 1–8.

Brandt, F., Bosbach, D., Krawczyk-Bärsch, E., Arnold, T. & Bernhard, G. 2003. Chlorite dissolution in the acid pH-range: a combined microscopic and macroscopic approach. *Geochimica et Cosmochimica Acta* 67(8): 1451–1461.

Byegård, J., Johansson, H. & Skålberg, M. 1998. The interaction of sorbing and non-sorbing tracers with different Äspö rock types—Sorption and diffusion experiments in the laboratory scale. Swedish Nuclear Fuel and Waste Management Co., Stockholm, Sweden, SKB Technical Report TR-98-18(Stockholm, Sweden).

Casey, W.H., Westrich, H.R., Arnold, G.W. & Banfield, J.F. 1989. The surface chemistry of dissolving labradorite feldspar. *Geochimica et Cosmochimica Acta* 53(4): 821–832.

Dubois, I.E., Holgersson, S., Allard, S. & Malmstrom, M.E. 2010. Dependency of BET surface area on particle size for some granitic minerals. (Submitted).

Gautier, J.-M., Oelkers, E.H. & Schott, J. 2001. Are quartz dissolution rates proportional to B.E.T. surface areas? *Geochimica et Cosmochimica Acta* 65(7): 1059–1070.

Gustafsson, Å., Molera, M. & Puigdomenech, I. 2004. Study of Ni(II) sorption on chlorite—a fracture filling mineral in granites. *Materials Research Society Symposium Proceedings* 824, art no CC7.3: 373–378.

Hamer, M., Graham, R.C., Amrhein, C. & Bozhilov, K.N. 2003. Dissolution of Ripidolite (Mg, Fe-Chlorite) in Organic and Inorganic Acid Solutions. *Soil Science Society of America Journal* 67: 654–661.

Hodson, M.E. 1999. Micropore surface area variation with grain size in unweathered alkali feldspars: Implications for surface roughness and dissolution studies. *Geochimica et Cosmochimica Acta* 62(21/22): 3429–3435.

Hodson, M.E. 2006. Does reactive surface area depend on grain size? Results from pH3, 25°C far-from-equilibrium flow-through dissolution experiments on anorthite and biotite. *Geochimica et Cosmochimica Acta* 70(7): 1655–1667.

Holdren, G.R.J. & Speyer, P.M. 1985. pH dependent changes in the rates and stoichiometry of dissolution of an alkali feldspar at room temperature. *American Journal of Science* 285: 994–1026.

Holdren, G.R.J. & Speyer, P.M. 1987. Reaction rate-surface area relationships during the early stages of weathering. II. Data on eight additional feldspars. *Geochimica et Cosmochimica Acta* 51(9): 2311–2318.

Krawczyk-Bärsch, E. et al. 2004. Formation of secondary Fe-oxyhydroxide phases during the dissolution of chlorite—effects on uranium sorption. *Applied Geochemistry* 19(9): 1403–1412.

Malmström, M., Banwart, S., Lewenhagen, J., Duro, L. & Bruno, J. 1996. The dissolution of biotite and chlorite at 25°C in the near-neutral pH region. *Journal of Contaminant Hydrology* 21(1–4): 201–213.

Rozalen, M. et al. 2008. Experimental study of the effect of pH on the kinetics of montmorillonite dissolution at 25°C. *Geochimica et Cosmochimica Acta* 72(17): 4224–4253.

White, A.F., Peterson, M.L. 1990. Role of Reactive-Surface-Area Characterization in Geochemical Kinetic Models, Chemical Modeling of Aqueous Systems II. ACS Symposium Series. American Chemical Society, Washington, DC, 461–475.

Zazzi, Å. 2009. Chlorite: Geochemical properties, Dissolution kinetics and Ni(II) sorption. Doctoral Thesis in Chemistry, TRITA-CHE Report 2009:9: KTH Chemical Science and Engineering. Royal Institute of Technology, KTH, Stockholm, Sweden.

Zazzi, Å., Malmstrom, M.E. & Wold, S. 2010. Dissolution rate and stoichiometry of two different chlorites as a function of pH. (In prep.).